

Infiltration of Meteoric and Sea Water into Deep Fault Zones during Episodes of Coseismic Events: A Case Study of the Nojima Fault, Japan

Aiming Lin^{1)*}, Natsumi Tanaka²⁾, Shin-ichi Uda³⁾ and Madhusoodhan Satish-kumar¹⁾

¹⁾ Faculty of Science, Shizuoka University

²⁾ Graduate School of Science and Technology, Kobe University

³⁾ Earthquake Research Center, Association for the Development of Earthquake Prediction

Abstract

Fluid infiltration into active faults and shear zones is usually studied in the middle to upper crustal environment. Circulating fluids deposit clay and carbonate material into cracks within the fault zone. Such crack-fill clay, calcite veins, and oxidized/weathered open cracks are well observed in the drill cores, from near-surface to a depth of 1,800 m, in the Nojima fault zone, Japan, which triggered the 1995 M7.2 Kobe earthquake. Powder X-ray diffraction analysis indicates that the crack-fill clay veins are mainly composed of siderite, calcite, laumontite, and fine-grained clasts of granitic rock. Isotopic analyses of carbonate material within the clay and calcite veins reveal variable $\delta^{18}\text{O}$ (SMOW) values ranging from 20.1‰ to 27.7‰, and $\delta^{13}\text{C}$ (PDB) values of -4.3‰ to -18.5‰, which are comparable to those of typical meteoric and sea water. ^{14}C dates of 10 clay and calcite vein samples range from 35.0 kyr B.P. to 58.4 kyr B.P.

Geological, petrological, stable isotopic, and ^{14}C data suggest that these crack-fill clay and calcite veins and brown-colored open cracks developed due to the repeated infiltration of O_2 - and CO_2 -bearing meteoric and sea water downward into the deep Nojima fault zone during the last 35-60 kyr. We propose a seismic fault suction pumping model to interpret the infiltration of subsurface waters being carried down into the deep fault zone by a rapid potential change during episodes of seismic faulting.

Key words: fluid infiltration, meteoric and sea water, active fault zone, seismic fault suction pumping model

1. Introduction

In the past two decades, increasing geological evidence has emerged that faults and shear zones within the middle to upper crust play a crucial role in controlling the architecture of crustal fluid migration (e.g. Kerrich *et al.*, 1984; Sibson *et al.*, 1988; Cox, 1995; Uda *et al.*, 1999), and that fluids migrating through faults have a substantial influence on fault mechanics (e.g. Sibson, 1992; Chester *et al.*, 1993; Evans and Chester, 1995). In particular, the potential weakness of major faults (e.g. San Andreas fault) has stimulated a discussion on the role of fluids in crustal faulting (see review by Hickman *et al.*, 1995). There

is, however, considerable debate concerning the source and the migration mechanism of fluids within faults: whether they originated from depths of the order of 5-20 kilometers (seismogenic zone) due to coseismic strain changes in the surrounding crust (e.g. Muir-Wood and King, 1993) or are largely the result of near-surface changes in failure permeability induced by strong ground motions (Rojstaczer and Wolf, 1992) or by groundwater potential changes caused by seismic faulting (Uda *et al.*, 1999). Potential sources of fluids in brittle fault and shear zones probably include metamorphic fluid generated by dehydration of minerals during prograde

*e-mail: slin@ipc.shizuoka.ac.jp (Ohya 836, Shizuoka 422-8529 Japan)

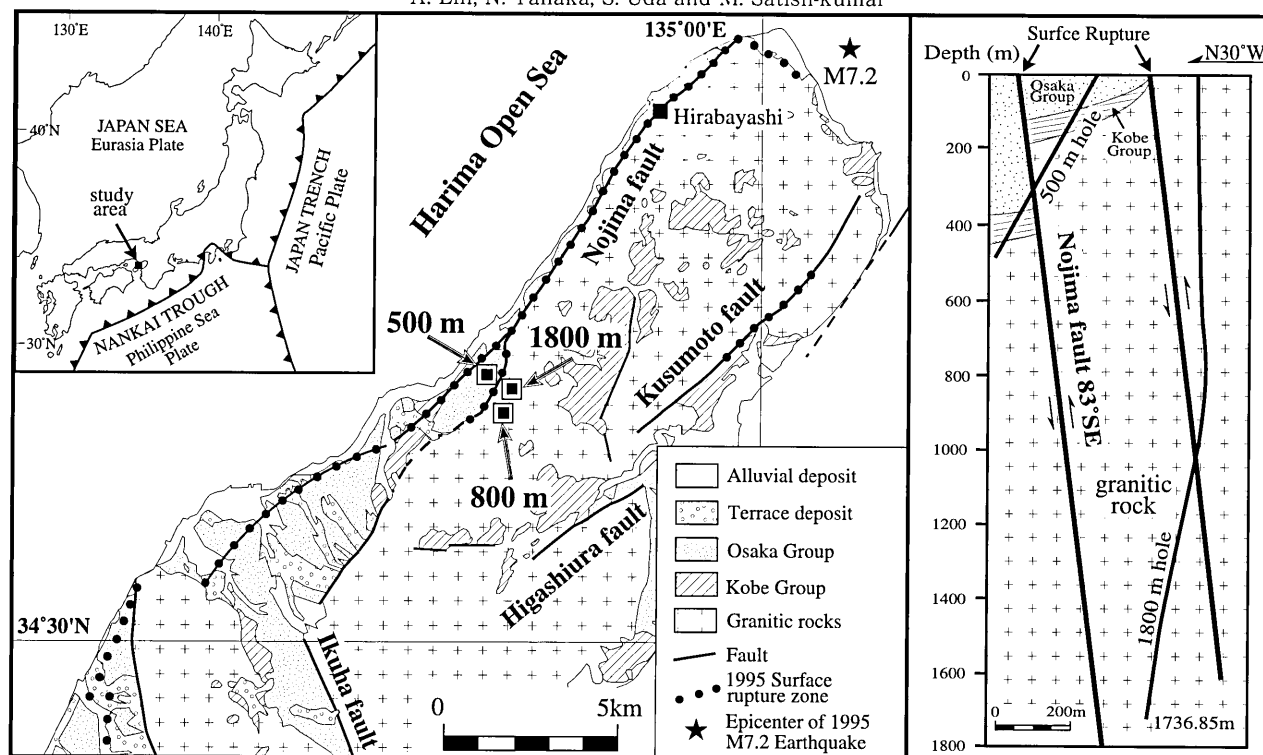


Fig. 1. Simplified geological map of northern Awaji Island, Japan (modified from Mizuno *et al.* 1990; Lin and Uda, 1996a, Lin *et al.*, 2001b) and geological section across the 500-m and 1,800-m drill hole sites. Solid squares: 500 m, 800 m, and 1,800 m, and Geological Survey of Japan (GSJ) Hirabayashi drill hole sites.

metamorphism (Etheridge *et al.*, 1984), meteoric water drawn into the fault zone in response to fault rupture by circulation (Kerrick *et al.*, 1984), and fluid trapped in pore spaces as sedimentary formation brines in the upper several kilometers of accretionary prisms in the forearc region (e.g. Bekins and Dreiss, 1992). Fluid exsolved from magma is another potential source, at least in certain thermal regions, there is isotopic and geochemical evidence that mantle-derived water and carbon dioxide may be upwelling along major crustal-penetrating faults (e.g. Kennedy *et al.*, 1997).

Recent studies investigating potential fluid sources have generally approached the problem by one of two methods: chemical and isotopic study of springs, seeps, and wells associated with faults (e.g. Tsunogai and Wakita, 1995; Kennedy *et al.*, 1997), or comprehensive analyses of the internal structures of fault zones and chemical composition of fault-zone materials (e.g. Evans and Chester, 1995; Janssen *et al.*, 1997; Uda *et al.*, 1999; Eichhubl and Boles, 2000). Active faults related to the seismotectonic activities are ideal for investigating the role of fluids during and after seismicity. In particular, fault zones that

traverse through hard crystalline rocks carry a lot of valuable information during fault activity because originally these rocks were impermeable. The Nojima fault, activated during the 1995 M7.2 Kobe (Japan) earthquake, provides a good scenario for studying fluid flow mechanisms. Preliminary studies of Uda *et al.* (1999) and Ueda *et al.* (1999) on crack-fill material and calcite veins from drill cores through the active Nojima fault suggested that meteoric and sea water infiltrated the fault zone during episodes of seismic events.

In this study, we follow up on the work of Uda *et al.* (1999, 2001) with an investigation of the microstructure, isotopic signature, composition, and ^{14}C dating of carbonate material from the Nojima fault zone, Japan. The aim is to determine the origin, timing, and mechanism of the infiltration of fluids within the deep fault zone. Three holes with depths of 500 m, 800 m, and 1,800 m depths were drilled by the University Project Group of Japan (UPGJ) to investigate the structures and the seismic faulting process of the Nojima fault immediately following the 1995 Kobe earthquake (Fig. 1). These three drill cores are subsequently referred to as the 500-m, 800-m, and

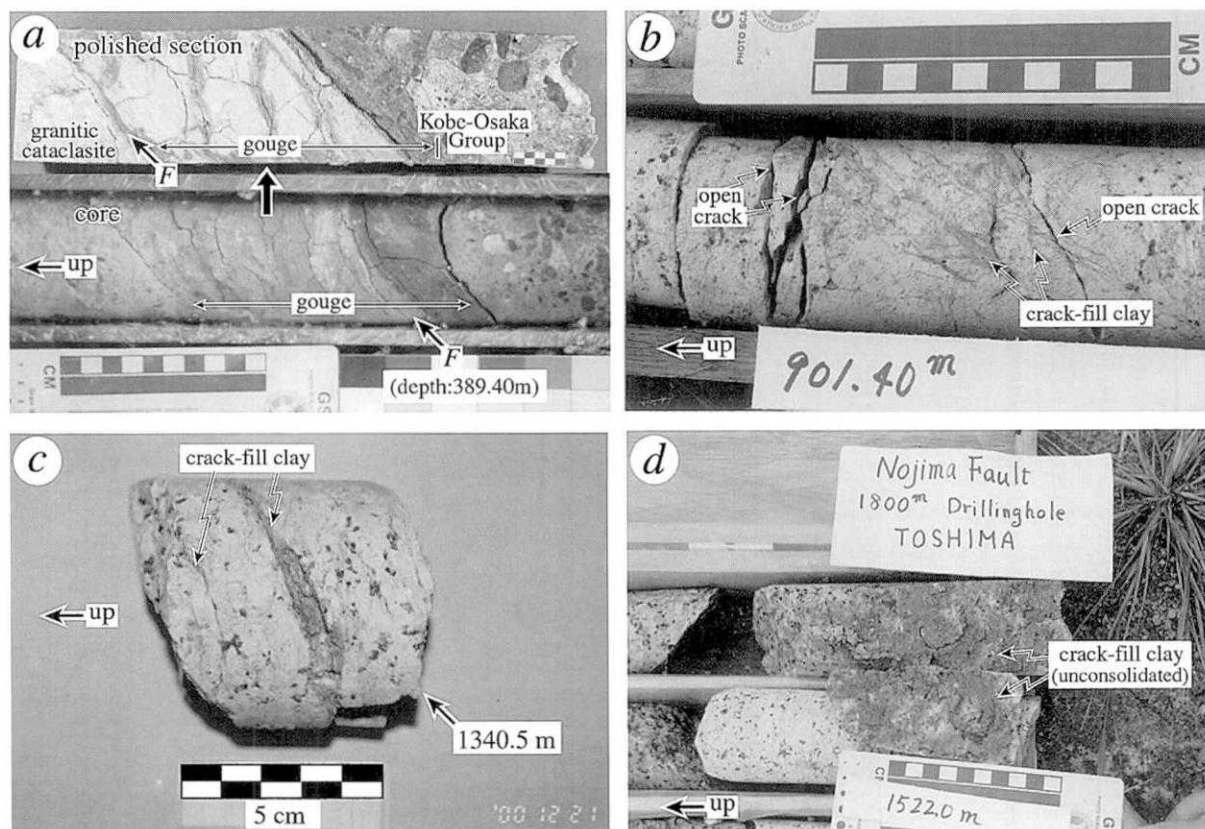


Fig. 2. Photographs showing the occurrences of the fault gouge in the 500-m core (a) and crack-fill clay veins and open cracks in the 1,800-m core (b-d). The crack-fill clay material is generally unconsolidated. Note that no obvious shearing-related fabric can be observed in the granitic wall rock adjacent to the open cracks.

1,800-m cores respectively. The two drill cores analyzed in this study comprise a section through a 15 cm-thick gouge-bearing fault at about 389 m (500 m hole) in depth, and a section through what may be the main fault at 1,800 m in depth. The drill core was previously described in detail by Kobayashi *et al.* (1999) and Lin *et al.* (2001).

2. Geological setting

The study area is located on the northern side of Awaji Island, southern Hyogo Prefecture, Japan (Fig. 1). The basement consists of pre-Neogene granitic rocks and the Miocene Kobe Group, which is unconformably overlain by the Plio-Pleistocene Osaka Group and late Quaternary alluvial and terrace deposits (Mizuno *et al.*, 1990). The Kobe Group is mainly composed of sandstone, conglomerate, sandy mudstone, and thin intercalated lignite beds. The Osaka Group is composed of weakly consolidated to unconsolidated beds of silt-clay, sand, and gravel.

Awaji Island is traversed by many active faults, most importantly the northeast-southwest striking

Nojima, Asano, Kusumoto, and Higashiura faults, and the northwest-southeast striking Ikuha fault (Fig. 1). These faults cut the Mio-Pleistocene Kobe-Osaka Groups and the Quaternary alluvial deposits (Research Group for Active Faults of Japan, 1991). Surface ruptures associated with the 1995 Kobe earthquake mainly developed along an 18-km section of the pre-existing Nojima fault zone (Lin and Uda 1995, 1996a,b; Lin, 1997). Prior to the 1995 event, the Nojima fault zone was 9 km in length and dipped 75° – 85° to the southeast (Fig. 1). The Nojima fault zone dextrally offsets late Quaternary alluvial fans and terraces by up to 30 meters with up to 10-meter vertical offsets. Average Quaternary slip rates along the Nojima fault are estimated to be 0.4–1.0 mm/y vertical, and 0.9–1.0 mm/y dextral (Mizuno *et al.*, 1990; Murata *et al.*, 2001).

Fault rocks in the fractured zone of the Nojima fault zone consist of foliated cataclasite, cataclasite, fault breccia, pseudotachylyte, and gouge (Lin, 1999, 2001; Lin *et al.*, 2001a). The granitic wall rock is medium-grained and is largely composed of quartz,

feldspar, and biotite, with minor hornblende (Lin *et al.*, 2001).

3. Occurrences of crack-fill clay, calcite veins, and open cracks

The 500-m drill hole was intended as a pilot hole to test the dip of the Nojima fault plane, and the 1800 m hole was subsequently drilled about 300 m south-east of the 500-m drill hole (Fig.1). The 1,800-m hole was actually terminated at 1,738 m due to difficulties in drilling through the fractured zone. Cores were taken at about 100 m intervals in this drill hole.

The 500-m and 1,800-m drill cores (called 500-m and 1,800-m cores, respectively) were observed immediately after coring to avoid later artificial disturbance and weathering, and were reobserved later in detail during this study. The 500-m cores are composed of the Kobe-Osaka Group sediments and granitic rock (Fig. 1). A 15-cm-thick gouge zone occurs at the main fault plane at a depth of 389.40 m (Fig. 2a) where granitic rock is thrust over Kobe-Osaka Group sediments. The entire 1,800-m core consists of granitic rock. Numerous open cracks are observed at all depths in both the 500-m and 1800-cores. Most of the open cracks are gray-yellow-brown to brown in color and filled by clay (Fig. 2b-d). The crack-fill clay (using the definition of Tsunoda *et al.* [1979]) occurs as single veins or complex networks of unconsolidated, and partially consolidated clay material (Fig. 2b-c), and consists of a lot of fine-grained clasts of granitic rock and calcite crystals (Fig. 3). The clay veins are generally 1-5 mm in width. No obvious shearing-related fabrics are recognized in the granitic rock adjacent to the cracks, which is generally hard and fresh in appearance. This suggests that the clay did not form due to in-situ shearing within the cracks, but due to the deposition of fine-grained material that was previously dissolved in or floating within an externally derived flowing fluid.

The calcite veins also occur as single veins or complex network veins, and are 1 mm to 2 cm in width and white to brown in color (Figs. 4-5a). Zoning textures in the veins are generally characterized by color laminations, and 1-mm to 3-cm cavities within the calcite veins also contain cyclic-zoning textures characterized by color laminations parallel to the cave wall (Fig. 5b-d). This indicates that the laminated calcite veins formed by multiple stages of

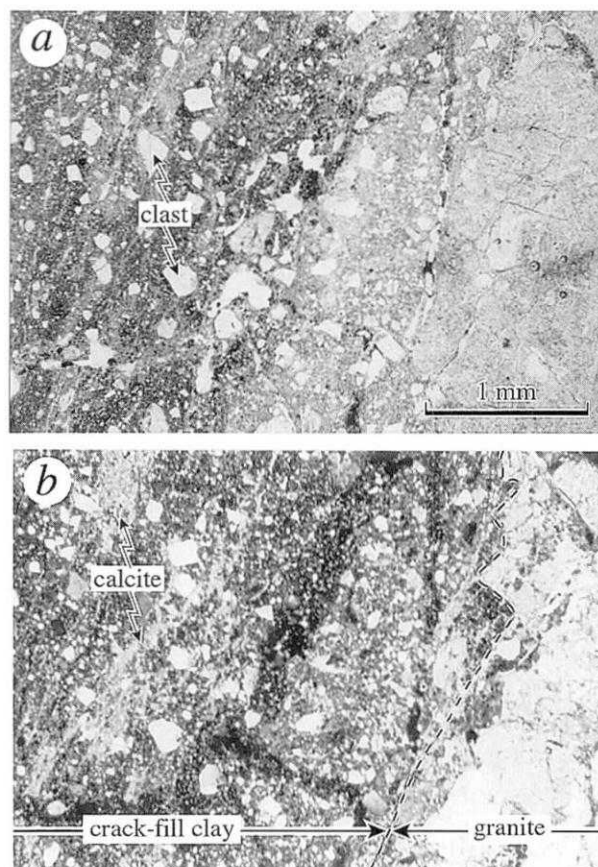


Fig. 3. Photomicrographs showing microstructures of the crack-fill clay veins. Numerous fine-grained clasts of granitic rock are included within the vein. Note that the boundary between the clay vein and the granitic wall rock is generally sharp. (a): plane-polarized light (PPL); (b): cross-polarized light (CPL).

fluid flow and the unfilled cavities remain the current conduits of fluid flow. Many open cracks are observed, which are yellow-brown to red-brown, similar to that of the crack-fill clay veins. The open cracks occur at all depths in both the 500-m and 1,800-m cores. There are no recognizable shearing-related textures in the granitic rock adjacent to the open cracks, although there are some hair-like cracks. This suggests that the open cracks developed due to dilatation under tensional stress and were subsequently oxidized by oxygen-rich fluids circulating through the cracks.

4. Powder X-ray analysis

An MXP SCIENCE X-ray diffractometer was used to identify minerals within the crack-fill clay veins. The experimental conditions were: filtered Cu K α (1.54050 Å) radiation, X-ray generator at 40 kV and 20

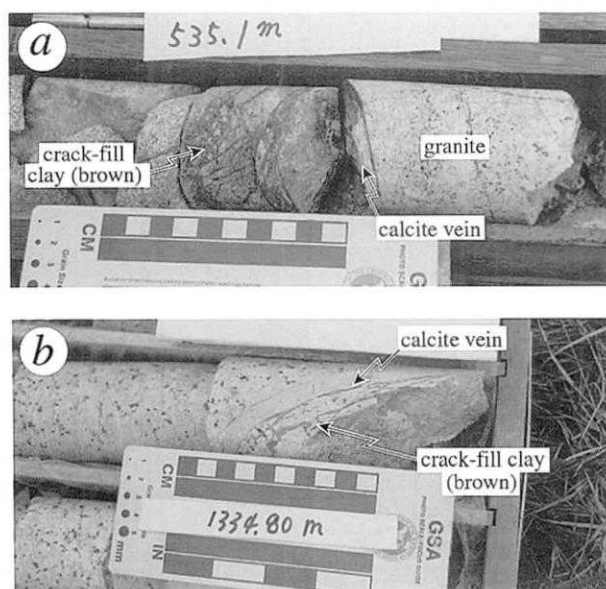


Fig. 4. Photographs showing occurrences of calcite and crack-fill clay veins. Note the brown crack-fill clay and white calcite veins co-exist in the same sample.

mA, divergence slit 1.0° , receiving slit 0.15 mm, scanning speed $2^\circ/\text{minute}$.

61 clay vein samples, taken from the top to the base of the 1,800-m core (Table 1), were prepared for powder X-ray diffraction analysis. To compare the mineral assemblages, samples of the granitic wall rock, fault gouge taken from the 500-m cores at the depth of 389.40 m and outcrops reported by Lin *et al.* (2001) were also analyzed. The bentonite used during drilling as clay materials of muddy-water to protect the wall of drill hole against collapse, was also analyzed to avoid the contamination of bentonite when identifying of mineral assemblages within the core samples.

Typical X-ray diffraction spectra are shown in Fig. 6. Crack-fill clay material is mainly composed of laumontite, smectite, siderite, calcite, and granitic rock-forming minerals such quartz, feldspar, and biotite, which are included in the veins as fine-grained

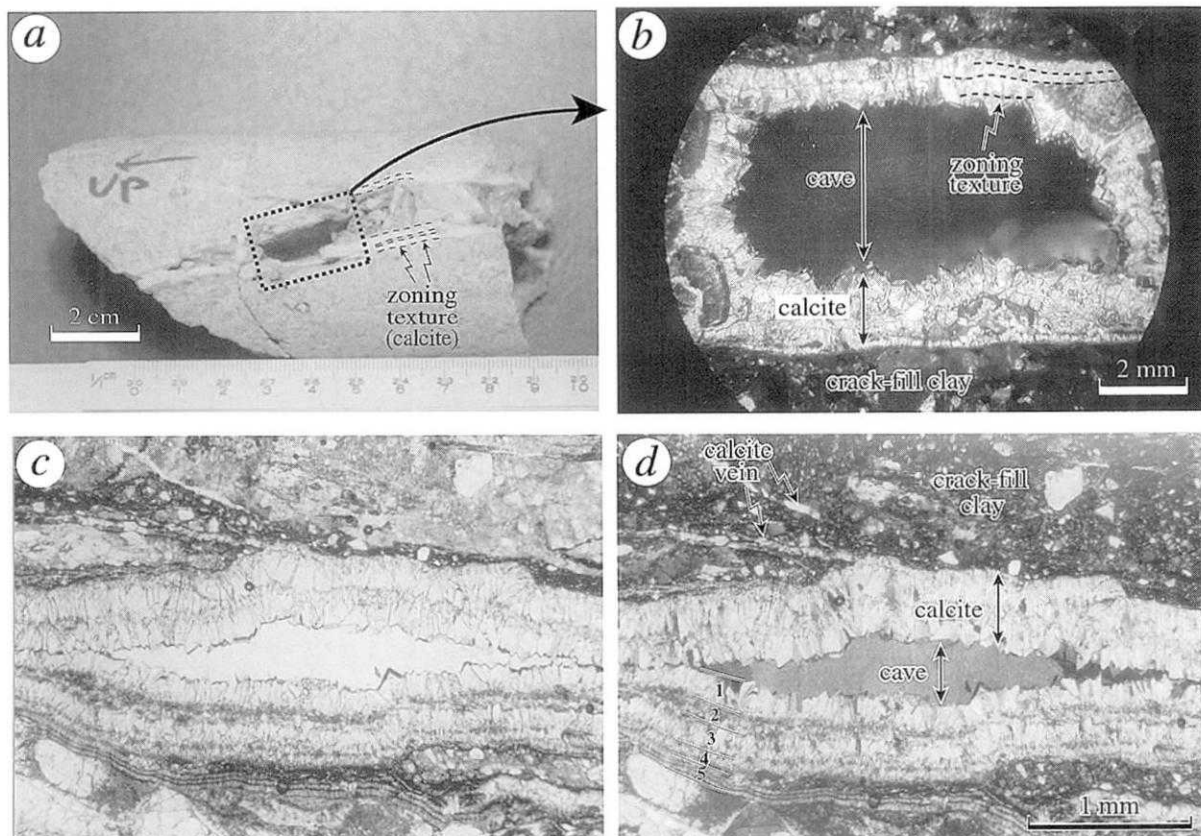


Fig. 5. Photograph (a) and photomicrographs (b-d) showing void cavities within the calcite vein and zoning textures observed in the calcite veins at depths of 384.10 m (a-b) and 463.0 m (c-d). (b) is the polished section of the area around the cavities shown in (a). Note that the open crack is not completely filled with clay or carbonate materials, which shows an elongated lens-shape cave structure within the calcite veins (c-d). Zoning textures found in the calcite veins are characterized by color laminations parallel to the cave wall (b-d). (b, d): CPL; (c): PPL.

Table 1. Mineral assemblages of crack-filling clay identified by power X-ray diffraction analysis. Qz: quartz, Pla: plagioclase, Ort: orthoclase, Bio: biotite, Horn: hornblende, Chl: chlorite, Smec: smectite, Lau: laumontite, Sti: Stilbite, Cal: calcite, and Sid: siderite. ⊙: strong crystal peak, ○: middle strong crystal peak, △: weak crystal peak, and -: no crystal peak or the crystal peak is too weak to be recognized.

sample no.	depth (m)	Qz	Pla	Ort	Bio	Horn	Chl	Smec	Lau	Sti	Cal	Sid
1	103.50	⊙	△	-	△	○	-	○	-	△	-	△
3	113.15	⊙	⊙	-	-	-	-	-	-	△	-	-
4	215.10	○	○	-	○	○	-	-	-	-	-	△
5	316.00	○	○	-	-	△	○	-	-	-	-	-
7	422.90	○	○	-	-	-	-	-	-	○	-	○
8	533.20	○	△	-	○	○	-	-	-	△	-	-
11	786.85	○	△	-	-	-	-	-	-	△	⊙	△
12	787.60	⊙	○	-	△	△	-	-	-	-	△	-
13	788.75	⊙	○	-	△	-	-	-	-	△	-	○
14	790.20	⊙	○	-	-	-	-	-	-	△	-	-
15	790.20	⊙	○	-	-	△	-	-	-	-	-	-
17	901.40	⊙	○	○	-	-	-	-	-	-	-	○
20	1276.80	○	△	-	-	-	-	-	○	-	○	⊙
21	1279.20	○	○	-	-	-	-	-	-	-	○	○
22	1284.20	△	△	-	-	-	-	-	○	-	△	⊙
23	1288.70	○	△	-	-	-	-	-	-	-	○	⊙
24	1294.80	-	-	-	-	-	-	-	⊙	-	⊙	-
25	1299.40	△	△	-	-	-	-	-	-	-	○	○
26	1303.55	○	△	-	-	-	-	-	-	-	○	○
27	1308.70	○	△	-	-	-	-	-	-	-	○	○
28	1314.40	○	△	△	-	-	-	-	-	-	○	○
29	1334.80	△	△	-	-	-	△	-	○	-	○	⊙
30	1390.10	○	○	△	-	-	-	-	-	-	-	-
31	1403.35	○	△	-	-	-	-	-	-	-	○	○
32	1416.30	○	○	△	-	-	-	-	-	-	-	△
33	1428.80	△	-	-	-	-	-	-	-	-	○	○
34	1437.00	○	○	-	△	-	-	-	-	-	○	△
35	1454.80	○	○	-	-	-	-	-	-	-	-	○
36	1469.25	○	△	-	-	-	-	-	-	-	○	○
37	1477.85	-	-	-	-	-	-	-	○	-	○	⊙
38	1495.95	⊙	○	△	-	-	-	-	-	-	-	○
39	1505.85	○	○	△	-	-	-	-	○	-	-	-
40	1507.20	○	△	-	-	-	-	-	-	-	-	-
41	1512.85	○	○	-	-	-	-	-	-	-	○	○
42	1518.30	○	△	-	-	-	-	-	-	-	-	○
43	1522.00	△	△	-	-	-	-	-	-	-	○	○
44	1528.30	○	△	△	-	-	-	-	○	-	-	-
45	1550.15	○	○	-	-	-	-	-	-	-	○	-
46	1555.30	○	○	-	-	-	-	-	-	-	-	○
47	1555.90	○	○	-	-	-	△	-	-	-	-	-
48	1567.75	○	○	-	-	-	-	-	-	-	-	-
49	1567.75	○	○	-	-	-	-	-	-	-	○	△
50	1574.15	○	△	-	-	-	-	-	-	-	△	△
51	1578.25	○	○	-	-	-	-	-	-	-	○	△
52	1597.10	○	○	-	-	-	-	-	-	-	-	○
53	1605.10	⊙	○	-	-	-	-	-	△	-	○	○
54	1624.15	○	○	-	-	-	-	-	-	-	△	○
55	1627.25	○	○	-	△	-	-	-	-	-	-	○
56	1635.45	⊙	○	-	△	-	-	-	-	-	-	-
57	1650.55	○	○	-	-	-	-	-	-	-	-	△
58	1658.35	⊙	○	-	-	-	-	-	-	-	-	○
59	1673.15	○	○	-	-	-	-	-	-	-	-	-
60	1700.15	○	○	-	△	-	-	-	-	-	○	△
61	1708.00	⊙	○	-	-	-	-	-	-	-	-	-

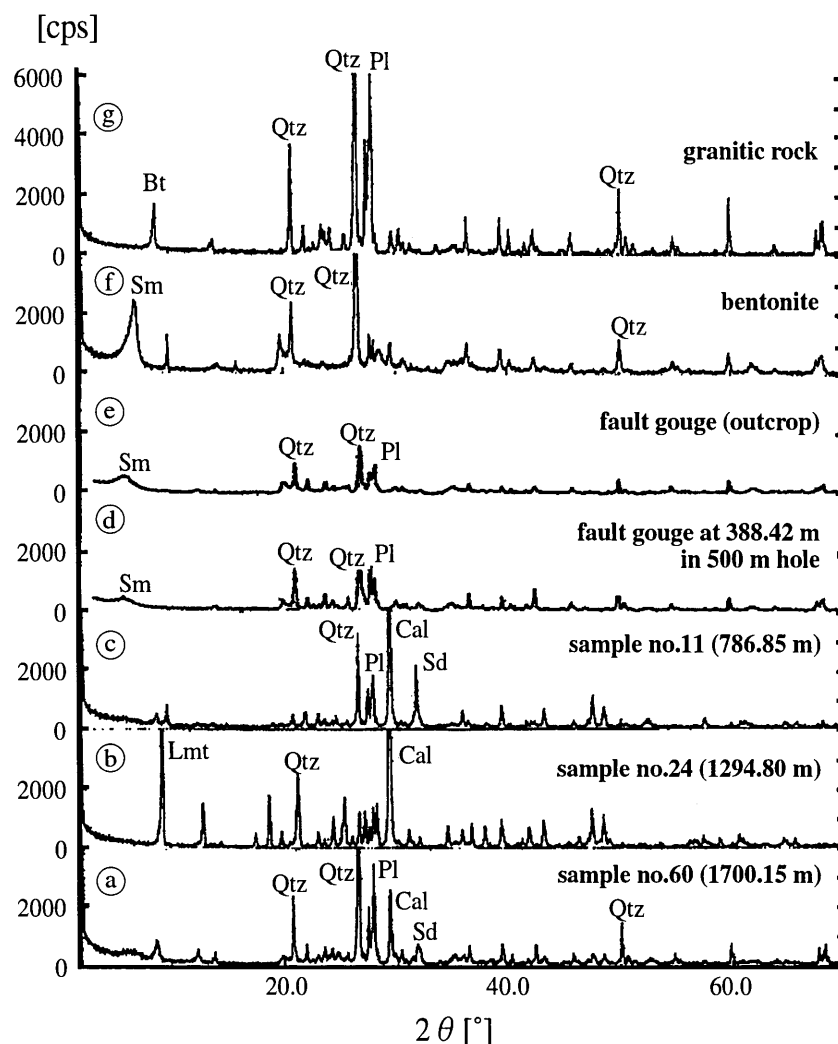


Fig. 6. Powder X-ray diffraction spectra of the crack-fill clay vein samples taken from the 1,800-m core (a-c), fault gouges taken from the 500-m core (d), and the outcrop (e), bentonite sample (f), and granitic rock (g). Qtz; quartz; Pl; plagioclase; Bt; biotite; Cal; calcite; Sm; smectite; Sd; siderite.

clasts derived from the granitic host-rock (Fig. 6, Table 1). The host granitic rock and the fault gouges consist mainly of quartz, feldspar, hornblende, and biotite, which are compositionally different from that of the crack-fill clay (Fig. 6). This indicates an external source for the crack-fill clay material.

5. Isotope analysis

Thirteen calcite-rich vein samples from various depths within the 1,800-m core were selected for $\delta^{13}\text{O}$ and $\delta^{13}\text{C}$ stable isotope analyses (Table 2). Pure calcite crystals were scraped with a knife from a polished slab of carbonate vein after observation under optical microscope using a thin section. Pulverized calcite was placed in a small stainless steel cup, which was put into a reaction vessel that contained concen-

trated phosphoric acid at 60 °C and under vacuum in order to liberate CO_2 (using method of Wada *et al.* [1984]). The liberated CO_2 gas was purified cryogenically and analyzed with a Finnigan MAT 250 mass spectrometer for carbon and oxygen isotopes. Isotopic data are reported as $\delta^{13}\text{O}$ and $\delta^{13}\text{C}$ values in the conventional delta notation in per mil relative to SMOW for oxygen and PDB for carbon (Figs. 7-8 and Table 2). The analytical results show that the $\delta^{13}\text{O}$ and $\delta^{13}\text{C}$ values of carbonate samples vary from 21.0‰ to 27.7‰, and -4.6‰ to -18.5‰, respectively.

6. ^{14}C dating of calcite veins

Ten calcite vein samples were selected for ^{14}C dating to determine the timing of crack-filling. ^{14}C dates were measured at the Tono Geoscience Center,

Table 2. Isotope compositions of carbonate samples taken from 1,800 m core.

sample No.	sample depth (m)	$\delta^{13}\text{C}$ (‰PDB)	$\delta^{18}\text{O}$ (‰SMOW)
1	786.85	-4.575 ± 0.021	20.855 ± 0.034
2	1267.70	-14.458 ± 0.014	27.668 ± 0.051
3	1294.80	-12.479 ± 0.017	20.321 ± 0.057
4	1299.40	-10.890 ± 0.018	20.543 ± 0.039
5	1323.60	-11.346 ± 0.036	20.990 ± 0.057
6	1340.05	-14.925 ± 0.045	25.659 ± 0.038
7	1458.50	-8.456 ± 0.020	21.896 ± 0.051
8	1477.85	-9.538 ± 0.042	22.297 ± 0.067
9	1484.40	-8.539 ± 0.030	21.839 ± 0.050
10	1522.00	-9.158 ± 0.027	20.899 ± 0.063
11	1575.85	-12.831 ± 0.024	22.659 ± 0.032
12	1624.15	-14.637 ± 0.040	22.832 ± 0.049
13	1700.15	-18.487 ± 0.015	24.128 ± 0.022

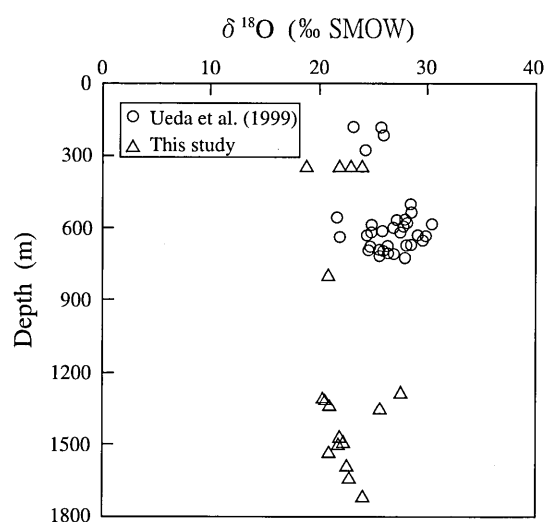


Fig. 7. Diagram showing the analytical results of $\delta^{18}\text{O}$ versus depth in the 1,800-m drill core. The data of Ueda *et al.* (1999) were obtained from the Hirabayashi drill core of GSJ (see Fig. 1 for locality).

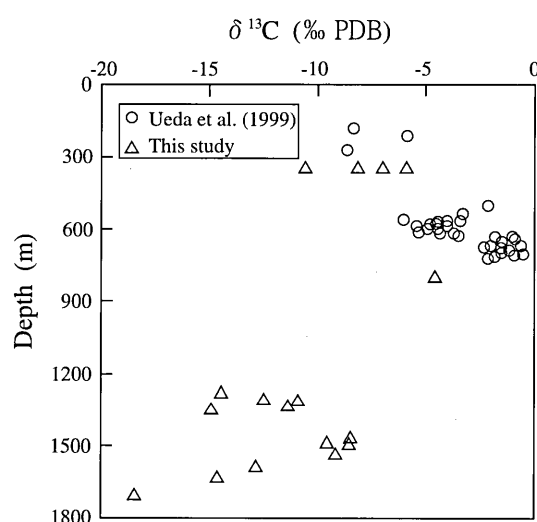


Fig. 8. Diagram showing the analytical results of $\delta^{13}\text{C}$ versus depth in the 1,800-m drill core. The data of Ueda *et al.* (1999) were obtained from the Hirabayashi drill core of GSJ (see Fig. 1 for locality).

Japan Nuclear Cycle Development Institute, and are presented in Fig. 9 and Table 3. The method involves liquid scintillation counting on synthesized benzene in a refrigerated Intertechnique SL-30 counter. Radiocarbon dates reported here are based on 95% activity of NBS oxalic acid and ANU sugar, using the Libby half-life ($5,568 \pm 30$ yr) with a two counting error including variations in sample and background. ^{14}C dating ages of calcite veins range from 34.96 ± 0.23 kyr B.P. to 58.43 ± 0.15 kyr. B.P. (Table 3).

7. Discussion

7.1. Source of fluids within the Nojima fault zone

The presence of crack-fill clay and calcite veins indicates the circulation of high Ca, CO_2 , and O_2 fluids within the Nojima fault zone. Chemical and isotopic analyses of carbonate veinlets within fault zones are commonly used to infer the origin of fluids within fault zones (e.g. Kerrich *et al.*, 1984; Janssen *et al.*, 1997; Kharaka *et al.*, 1999; Ueda *et al.*, 1999). The isotopic values of fluids in chemical equilibrium with the calcite at various depths were calculated using the equilibrium equations of O'Neil *et al.* (1969) for $\delta^{18}\text{O}$ under the temperatures measured inside the

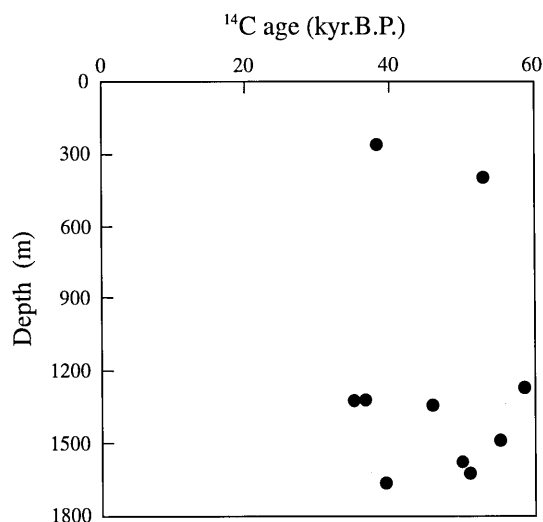


Fig. 9. ^{14}C ages of carbonate veins versus depth in the 1800 m core.

Table 3. ^{14}C dating results of carbonate samples taken from 1,800 m core.

sample no.	depth (m)	^{14}C age (yr.B.P.)
01	258.03	$38,132 \pm 318$
02	389.40	$52,940 \pm 1,279$
03	1267.75	$58,431 \pm 1,535$
04	1318.40	$36,510 \pm 264$
05	1323.60	$34,955 \pm 232$
06	1340.10	$45,660 \pm 573$
07	1484.40	$54,949 \pm 1,491$
08	1575.90	$49,787 \pm 625$
09	1624.15	$50,872 \pm 991$
10	1665.20	$39,241 \pm 367$

1,800-m drill core (geothermal gradient of $30^\circ\text{C}/\text{km}$, Yamano and Goto, 1998) and are plotted in Fig. 10. These results show that the $\delta^{18}\text{O}$ values of the carbonate veins are comparable to those of sea water and typical Japanese meteoric water, but are different from that of mantle-derived water (Fig. 10). The $\delta^{13}\text{C}$ values of carbonate material are similar to that of atmospheric CO_2 , marine plants, and sedimentary rocks, but are different from mantle-derived carbon and deep ocean carbonate (Fig. 11). These results indicate that the carbonate-rich veins formed from fluids that originated mainly from sea water, possibly mixed with meteoric water.

The difference of mineral assemblage between the crack-fill clay material and the fault gouge (Fig. 6) indicates that the rock-fill clay material was not generated inside the cracks by a shearing of the host granitic rock. It has been demonstrated that siderite

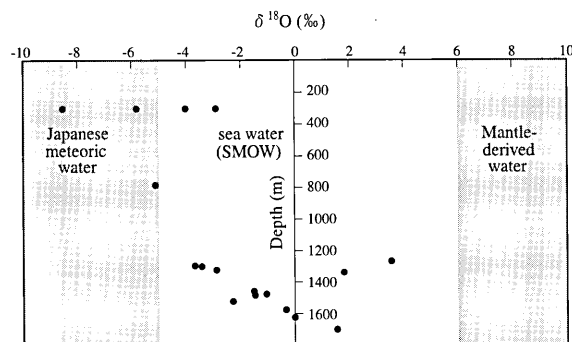


Fig. 10. Diagram showing the $\delta^{18}\text{O}$ values of sea water (SMOW), meteoric water (data from Matsuo, 1997) and the calculated results of $\delta^{18}\text{O}$ values of carbonate veins measured in this study in chemical equilibrium fluids with the carbonate materials using temperatures measured inside drill hole.

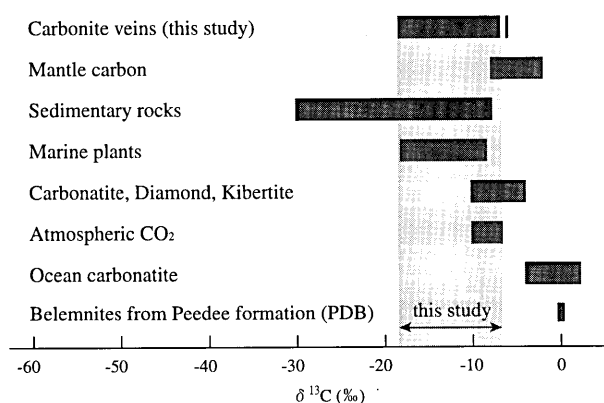


Fig. 11. Diagram showing the $\delta^{13}\text{C}$ values (PDB) of typical mantle-derived carbon, marine plants, sedimentary rocks, atmospheric CO_2 (data from Matsuo, 1997) and carbonate veins measured in this study. The $\delta^{13}\text{C}$ values of carbonate material are similar to that of atmospheric CO_2 , marine plants, and sedimentary rocks but different from mantle-derived carbon and deep ocean carbonate.

generally forms under conditions of lower Eh (oxidation potential) (Garrels and Christ, 1965). The groundwater near the Nojima fault contains large amounts of HCO_3^- (Sato and Takahashi, 1997), and high concentrations of CO_2 and H_2 were detected in the 1,800-m drill hole (Arai *et al.*, 1998). This CO_2 -rich fluid is not mantle- or magma-derived, but is probably formed by a chemical reaction of meteoric O_2 and CO_2 within the groundwater in the upper zone, which is shallower than the stable groundwater level (Arai *et al.* 1998). We suggest, therefore, that the crack-fill clay material and brown-colored open cracks containing siderite (FeCO_3) and calcite (CaCO_3) were

generated by the reaction of Ca and HCO_3 or CO_2 , originating from surface waters (meteoric and sea water), which were circulated in the fault zone.

The cracks developed at shallow depths are generally weathered, eroded, and oxidized by oxygen-rich groundwater including meteoric and sea water. The open cracks presented in the shallow zone around the stable groundwater level generally at depths < 100 m in Japan, which are usually filled by clay and calcite material and brown-colored as described above, and are generally formed by the oxidation of Fe, because where there is a rich oxygen content in groundwater circulating in the fault zone (Uda *et al.*, 1999). In general, cracks within deep fault zone remain unoxidized due to anoxic conditions at depth. The distribution depth of brown-colored cracks is commonly used as an indicator of stable groundwater level during hydrogeologic investigation. It was found, however, that many brown-colored open cracks occur in the 1,800 m core at all depths, although the stable groundwater level less than 6 m at the drill site (Uda *et al.*, 1999). This indicates that considerable volumes of oxygen-rich water were drawn into the fault zone to depths of > 1,800 m and oxidized the open cracks.

The calcite materials usually occur in reactivated parts of cracks as a coating on earlier crack-fill carbonate materials. The co-existence of unconsolidated crack-fill clay and consolidated calcite veins shows that they formed during a multi-stage process by repeated infiltration events. The newly-formed carbon materials included in flowing water were probably contaminated or mixed with the pre-existing fluids containing dead- or old-carbon and were deposited on the pre-existing carbonate materials. It is impractical to separate the new- and old-carbonate material for ^{14}C dating. Therefore, the age determined from the carbonate materials probably indicates a mixed age of multi-stages, which is usually older than the age of the last carbonate material deposition. We suggest that the deposition of carbonate material in the open cracks took place repeatedly during the last 30-60 kyr, primarily by the infiltration of meteoric and sea water into the Nojima fault zone (see below detail). The colored laminae (zoning textures) of calcite veins also show they formed by multi-stages of flowing fluids, which support that the variable ^{14}C dating ages determined from the calcite

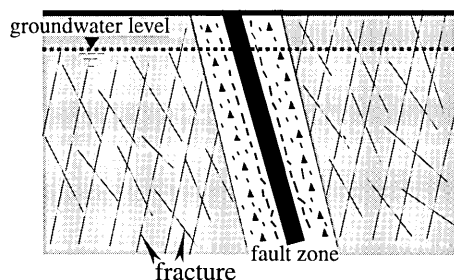
veins reflect the repeated events of carbonate formation.

7.2. Mechanism of surface water infiltration deep into the active fault zone

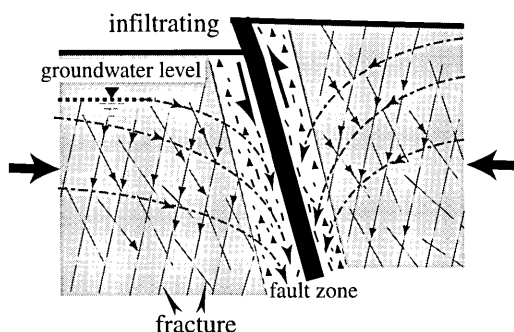
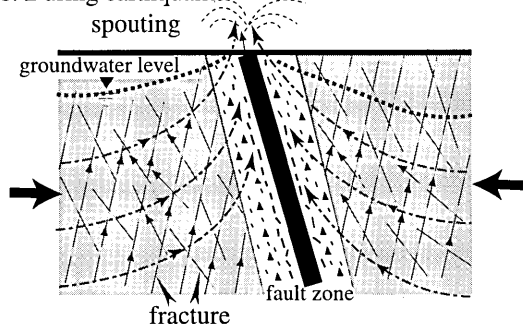
The accumulated evidence suggests that the CO_2 - and O_2 -rich surface waters, including meteoric and sea water, infiltrated repeatedly into the Nojima fault zone. The groundwater level measured inside drill holes penetrating the Nojima fault zone is < 6 m (Uda *et al.*, 1999), and the depth of the sea floor around Awaji Island is < 150 m (Lin and Uda, 1996b). Thus it is unlikely that groundwater including meteoric and sea water infiltrated to depths of > 1,800 m due to the seasonal fluctuation of groundwater level. The question is how did the surface waters infiltrate deep into the fault zone? A consequence of the dilatancy/fluid-diffusion mechanism for shallow earthquakes is that considerable volumes of fluid are rapidly redistributed in the crust following seismic faulting, which is borne out by outpourings (Sibson *et al.*, 1975) and falling of groundwater level along fault traces following some moderate to large earthquakes (e.g. Touda *et al.*, 1995; Osada *et al.*, 1997; Huang *et al.*, 1999). Groundwater fluctuation during earthquake events has been observed during recent strong earthquakes (e.g. Touda *et al.*, 1995; Huang *et al.*, 1999). It was reported that the outpouring and falling of groundwater occurred in many localities along the Nojima fault zone during the 1995 Kobe earthquake (Touda *et al.*, 1995), and that the groundwater level measured inside boreholes 4 months after the earthquake is about 2 m lower than that measured before the earthquake (Japan Society of Engineering Geology, 1996). The lowering of groundwater level during the 1999 M7.8 Chi-Chi (Taiwan) earthquake was up to 11 m on the day before the earthquake in the foot wall along and around the 100 km-long Chelungpu surface rupture zone (Lin *et al.*, 2001b) where many outpourings occurred (Huang *et al.*, 1999). These observations indicate that the fluctuation of groundwater potential in and around the fault zones was caused by crustal deformation during large earthquakes. Accordingly, a fault suction pumping model is proposed to explain the formation mechanism of the infiltration of surface water downward into the deep fault zone to generate the crack-fill clay and calcite veins, and to oxidize and weather

Fault Pumping Model

a. Before earthquake



b. During earthquake



c. After earthquake

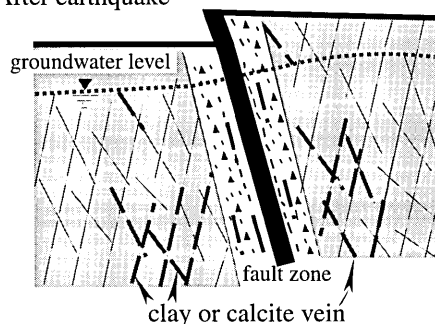


Fig. 12. Seismic fault suction pumping model.

the open cracks (Fig. 12). In contrast to the seismic pumping model of Sibson *et al.* (1975), we observed the phenomena that the meteoric and sea water-originated carbonate materials deposited in the deep fault zone, suggesting a suction mechanism that could cause a raising and a falling of groundwater

level to promote the circulation and infiltration of meteoric and sea water into the deep fault zone due to rapid potential changes of groundwater. The dilatancy/fluid-diffusion model of Scholz *et al.* (1973) provides an explanation for the intermittent flow of hydrothermal fluids in and around fault zones, and suggests that seismic faulting acts as a pumping mechanism, whereby individual earthquakes are capable of moving significant quantities of fluids from one crustal environment to another (Sibson *et al.*, 1975). As documented above, it is difficult for groundwater including meteoric and sea water to infiltrate to depths of $>1,800$ m due to seasonal fluctuations of groundwater level. Thus, we suggest that the mechanics of seismic faulting also play a vacuum suction pumping role and cause a high groundwater potential to draw down meteoric and sea water deep into the fault zone (Fig. 12).

A number of laboratory and field studies show that seismogenic faulting is substantially affected by the mechanical and chemical interaction of fluids and rocks (e.g. Evans and Chester, 1995; Tsunogai and Wakita, 1997). That discharging phenomena are often found in the epicentral area is probably due to this. After a strong earthquake, the fractured zone is restored to its strength state, and groundwater is also be restored its usual stable level from a funnel shape (Fig. 12). The O_2 - and CO_2 -bearing groundwater, therefore, would be drawn down into the deep fault zone by the vacuum pumping action or high groundwater potential during the restoration process as shown in Fig. 12.

8. Summary

Crack-fill clay and calcite veins and oxidized/ weathered open cracks are found in the active Nojima fault zone to a depth of 1,800 m. Petrological, isotopic, and ^{14}C data indicate that these veins and brown-colored open cracks probably formed due to infiltration of O_2 - and CO_2 -bearing meteoric and sea water downward into the deep fault zone during the last 35–60 kyr. We propose a seismic fault suction pumping model to interpret that the infiltration of surface waters as being carried down into a deep fault zone by rapid potential changes of groundwater during episodes of seismic faulting. This study presents an example of repeated infiltrations of meteoric and sea water deep into fault zones probably occur-

ring during seismic events.

Acknowledgements

We thank Professors T. Shimamoto of Kyoto University and T. Wada of Shizuoka University for their constructive discussions. We are grateful to Dr. A. Stallard for improving the English of the manuscript. This work is supported by the Science Research Project No.12440138 of the Ministry of Education, Culture, Sport, Science and Technology of Japan (for A. Lin) and partially by the Disaster Prevention Research Institute, Kyoto University.

References

- Arai, T., T. Okusawa and H. Tsukahara, 1998. Variation with depth in chemical composition and carbon isotope ratio of gas extracted from drilling cores. *Chikyū Monthly* No. 21, 165-170.**
- Bekins, B.A. and A. Dreiss, 1992. A simplified analysis of parameters controlling dewatering in accretionary prisms. *Earth Planet. Sci. Lett.* **109**, 275-287.
- Chester, F.M., J.P. Evans and R.L. Biegel, 1993. Internal structure and weakening mechanisms of the San Andreas Fault. *J. Geophys. Res.* **98**, 771-786.
- Cox, S.F., 1995. Faulting processes at high fluid pressures: an example of fault valve behavior from the Wattle Gully fault, Victoria, Australia. *J. Geophys. Res.* **100**, 21841-21859.
- Evans, J.M. and F.M. Chester, 1995. Fluid-rock interaction in faults of the San Andreas system: inferences from San Gabriel fault rock geochemistry and microstructures. *J. Geophys. Res.* **100**, 13007-13020.
- Etheridge, M.A., V.J. Wall, S.F. Cox and R.H. Vernon 1984. High fluid pressures during regional metamorphism and deformation: implications for mass transport and deformation mechanisms. *J. Geophys. Res.* **89**, 4344-4358.
- Eichhubl, P., and J.R. Boles, 2000. Focused fluid flow along faults in the Monterey formation, coastal California. *Geol. Soc. Am. Bull.* **112**, 1667-1679.
- Garrels, R.M., and C.L. Christ, 1965. Solutions, Minerals, and Equilibria. Harper & Row, New York, pp. 450.
- Hickman, S., R. Sibson, and R. Bruhn, 1995. Introduction to special section: Mechanical involvement of fluids in faulting. *J. Geophys. Res.* **100**, 12831-12840.
- Huang, C-Y., C-W. Lin, W-S. Chen, Y-G. Chen, S-B. Yu, I-P. Chia, M-D. Lu, C-S. Hou, and Y-S. Wang, 1999. Seismic geology of the Chi-Chi earthquake. In Huang *et al.* (eds) Field trip guide to seismic geology, International Workshop on the Taiwan Chi-Chi earthquake of September 21, 1999. p. 1-11.
- Japan Society of Engineering Geology (ed), 1996. Groundwater fluctuation caused by the earthquake. *Engineering Geology, J. Japan Soc. Engineer. Geol.* **37**, 351-358.
- Janssen, C., W. Michel, M. Bau, V. Lüders, and K. Mühle, 1997. The North Anatolian fault zone and the role of fluids in seismogenic deformation. *J. Geol.* **105**, 387-403.
- Kennedy, B.M., Y.K. Kharaka, W.C. Evans, A. Elwood, D.J. DePaolo, J. Thordsen, G. Ambats, and R.H. Mariner, 1997. Mantle fluids in the San Andreas fault system, California. *Science* **278**, 1278-1281.
- Kerrich, R., T.E. La Tour, and L. Willmore, 1984. Fluid participation in deep fault zones: evidence from geological, geochemical, and $^{18}\text{O}/^{16}\text{O}$ relations. *J. Geophys. Res.* **89**, 4331-4343.
- Kharaka, Y.K., J.J. Thordsen, and W.C. Evans, 1999. Geochemistry and hydromechanical interactions of fluids associated with the San Andreas Fault System, California. In Haneberg *et al.* (eds): Faults and surface fluid flow in the shallow crust, Geophysics Monograph, American Geophysical Union, **113**, p. 129-145.
- Kobayashi, K., T. Fukuchi, N. Hasebe, A. Lin, T. Maruyama, T. Matsuda, A. Murata, M. Shigetomi, K. Shimata, K. Takemura, H. Tanaka, N. Tanaka, N. Tomida, M. Toyota, S. Uda, and S. Yamakita, 1999. Occurrence of the marginal fracture zone in the 1,800 m drill core penetrating throughout the Nojima fault. *J. Geol. Soc. Japan* **105**, XIX-XX.**
- Lin, A., 1997. Instantaneous-shaking liquefaction induced by the M7.2 Southern Hyogo Prefecture earthquake, Japan. *Geology* **25**, 435-438.
- Lin, A., 1999. S-C cataclasis in granitic rock. *Tectonophysics* **304**, 257-273.
- Lin, A., 2001. S-C fabrics developed in cataclastic rocks from the Nojima fault zone, Japan and their implications for tectonic history. *J. Struct. Geol.* **23**, 1167-1178.
- Lin, A., and S. Uda, 1995. Segmentation and rupture propagation of the Nojima earthquake fault. *Zisin, J. Seismol. Soc. Japan* **48**, 375-86.*
- Lin, A., and S. Uda, 1996a. Morphological characteristics of the earthquake surface ruptures on Awaji Island, associated with the 1995 Southern Hyogo Prefecture Earthquake. *The Island Arc* **5**, 1-15.
- Lin, A., and S. Uda, 1996b. Tectonic history of the Akashi strait and the fault model associated with the Southern Hyogo Prefecture Earthquake. *J. Japan Soc. Engineer. Geol.* **37**, 160-171.*
- Lin, A., O. Ouchi, A. Chen, and T. Maruyama, 2001a. Co-seismic displacements, folding and shortening structures along the Chelungpu surface rupture zone occurred during the 1999 Chi-Chi (Taiwan) earthquake. *Tectonophysics* **330**, 225-244.
- Lin, A., T. Shimamoto, T. Maruyama, T. Shigetomi, T. Miyata, K. Takemura, H. Tanaka, S. Uda, and A. Murata, 2001b. Comparative study of the cataclastic fault rocks found in a core and outcrops along the Nojima fault in Awaji Island, Japan. *The Island Arc* **10**, 368-380.
- Matsuo, S., 1997. Geochemistry. Koudansha Scientific Co. Ltd., Tokyo, pp. 265.**
- Mizuno, K., H. Hattori, A. Sangawa, and Y. Takahashi, 1990. Geology of Akashi district, Quadrangle series, Okayama 9, 1 : 50,000 (12), No. 83, p. 90.*
- Muir-Wood, R., and G.C.P. King, 1993. Hydrological signatures associated with earthquake strain. *J. Geophys. Res.* **98**, 22035-22068.
- Murata, A., K. Takemura, T. Miyata, and A. Lin, 2001. Vertical displacement and average slip rate of the Nojima fault. *The Island Arc* **10**, 360-367.
- O'neil, J.R., R.N. Clayton, and T.K. Mayeda, 1969. Oxygen isotope fractionation in divalent metal carbonates. *J.*

- Chem. Phys.* **51**, 5547-5558.
- Osada, T., T. Tokugawa, H. Ichibashi, and T. Kayaki, 1997. Groundwater fluctuations in the northern part of Awaji Island after Hyogoken-Nanbu Earthquake. Annual meeting Abstract, *Japan Soc. Engineer. Geol.* 237-240.**
- Research Group for Active Faults of Japan, 1991. Active faults in Japan: sheet maps and inventories. The University of Tokyo Press, Tokyo, pp. 437.*
- Rojstaczer, S., and S. Wolf, 1992. Permeability changes associated with large earthquakes: An example from Loma Prieta, California. *Geology* **20**, 211-214.
- Sato, T. and M. Takahashi, 1997. Geochemical changes in anomalously discharged groundwater in Awaji Island after the 1995 Kobe earthquake. *Chikyukagaku* (Geochemistry) **31**, 89-98.*
- Scholz, C.H., L.R. Sykes, and Y.P. Aggarwal, 1973. Earthquake prediction: a physical basis. *Science* **181**, 803-811.
- Sibson, R.H., 1992. Implications of fault-valve behavior for rupture nucleation and recurrence. *Tectonophysics* **211**, 283-293.
- Sibson, R.H., J.McM. Moore, and A.H. Rankin, 1975. Seismic pumping-a hydrothermal fluid transport mechanism. *J. Geol. Soc. London* **131**, 653-659.
- Sibson, R.H., F. Robert, and K.H. Poulsen, 1988. High-angle reverse faults, fluid-pressure cycling, and mesothermal gold-quartz deposits. *Geology* **16**, 551-554.
- Touda, S., K. Tanaka, M. Chikira, K. Miyakawa, and T. Hasegawa, 1995. Coseismic behavior of groundwater by the 1995 Hyogo-ken Nanbu Earthquake. Zisin, *J. Seismol. Soc. Japan* **48**, 547-553.*
- Tsunoda, T., K. Miyakoshi, and M. Ogata, 1979. Crack-filling clay in fault fractured zone. Annual meeting Abstract, *Japan Soc. Engineer. Geol.* p. 56-59.
- Tsunogai, U., and H. Wakita, 1995. Precursory chemical changes in ground water: Kobe earthquake, *Japan. Science* **269**, 61-63.
- Uda, S., A. Lin, and K. Takemura, 1999. Deep surface-water flow near the Nojima earthquake fault. In Ito *et al.* (eds) : Proceedings of the international workshop on the Nojima fault core and borehole data analysis. *Geol. Surv. Japan Interim Report*, no.EQ/00/1, p. 193-202.
- Uda, S., A. Lin, and K. Takemura, 2001. Crack-filling clays and weathered cracks in the DPRI 1,800 m cores near the Nojima fault, Japan: evidence for deep surface-water circulation near an active fault. *The Island Arc* **10**, 439-446.
- Ueda, A., A. Kawabata, H. Koichiro, H. Tanaka, N. Tomida, T. Ohtani, and H. Ito, 1999. Isotopic study of carbonates in Nojima Fault cores. In Ito *et al.* (eds): Proceedings of the international workshop on the Nojima fault core and borehole data analysis. *Geol. Surv. Japan Interim Report*, no.EQ/00/1, p. 127-132.
- Wada, H., N. Fujii, and N. Niitsuma, 1984. Analytical method of stable isotope for ultra-small amounts of carbon dioxide with MAT-250 mass spectrometer. *Geoscience Reports of Shizuoka University* **10**, 103-112.*
- Yamano, M., and H. Goto, 1998. Long-term temperature measurement inside the Nojima fault drill hole. *Chikyu Monthly* No. 21, 102-107.**
- * in Japanese with English abstract
- ** in Japanese

(Received July 9, 2001)

(Accepted September 15, 2001)